Protein Science (1998), 7:1469–1476. Cambridge University Press. Printed in the USA.

Guanidine hydrochloride unfolding of a transmembrane β-strand in FepA using site-directed spin labeling

CANDICE S. KLUG AND JIMMY B. FEIX

Biophysics Research Institute, Medical College of Wisconsin, 8701 Watertown Plank Road, Milwaukee, Wisconsin 53226

(RECEIVED December 30, 1997; ACCEPTED February 13, 1998)

Abstract

We have used the electron spin resonance (ESR) site-directed spin-labeling (SDSL) technique to examine the guanidine hydrochloride (Gdn-HCl) induced denaturation of several sites along a transmembrane β-strand located in the ferric enterobactin receptor, FepA. In addition, we have continued the characterization of the β-strand previously identified by our group (Klug CS et al., 1997, *Biochemistry 36*:13027–13033) to extend from the periplasm to the extracellular surface loop in FepA, an integral membrane protein containing a β-barrel motif comprised of a series of antiparallel β-strands that is responsible for transport of the iron chelate, ferric enterobactin (FeEnt), across the outer membrane of *Escherichia coli* and many related enteric bacteria. We have previously shown that a large surface loop in FepA containing the FeEnt binding site denatures independently of the β-barrel domain (Klug CS et al., 1995, *Biochemistry 34*:14230–14236). The SDSL approach allows examination of the unfolding at individual residues independent of the global unfolding of the protein. This work shows that sites along the β-strand that are exposed to the aqueous lumen of the channel denature more rapidly and with higher cooperativity than the surface loop, while sites on the hydrophobic side of the β-strand undergo a limited degree of noncooperative unfolding and do not fully denature even at high (e.g., 4 M) Gdn-HCl concentrations. We conclude that, in a transmembrane β-strand, the local environment of a given residue plays a significant role in the loss of structure at each site.

Keywords: ESR; FepA; Gdn-HCl unfolding; membrane protein stability; SDSL; transmembrane β-strand

The electron spin resonance (ESR) site-directed spin-labeling (SDSL) technique has recently emerged as a powerful method for observing molecular motion at individual sites within a large protein structure (reviewed by Hubbell & Altenbach, 1994). SDSL is particularly useful for the study of membrane proteins, which often are not amenable to structural analysis by NMR methods (reviewed by Feix & Klug, 1997). And, unlike many other methods, such as circular dichroism (CD), fluorescence, and UV-vis absorbance, which allow only the monitoring of global changes in protein structure, SDSL allows the direct probing of the local environment and structure of individual residues. This is accomplished by substituting a cysteine residue at the site of interest and attaching a sulfhydryl-specific spin label such as methanethiosulfonate (MTSL, Fig. 6). The spin label adds minimal perturbation to the system, as it is approximately the size of a tryptophan residue. In addition, numerous studies of the effects of single mutations on the T4 lysozyme structure have been carried out and show that most mutations retain structural properties similar to the wild-type protein (work reviewed by Matthews, 1995).

Solvent-induced unfolding of proteins can provide insights into the overall stability of the protein, mechanisms of unfolding, and tertiary interactions between domains. Many studies have been carried out on the guanidine-HCl (Gdn-HCl) unfolding of globular proteins to obtain free energies of unfolding (ΔG_U), a quantitation of the overall protein stability (Pace & Vanderburg, 1979; Ahmad & Bigelow, 1982; Ho & DeGrado, 1987; Regan & DeGrado, 1988; Mücke & Schmid, 1994; Kragelund et al., 1995; Yao & Bolen, 1995). Although extensive literature exists on the denaturant unfolding of soluble proteins, few studies have been carried out on the denaturation of membrane proteins (Oikawa et al., 1985; Hill et al., 1988; Klug et al., 1995; Lau & Bowie, 1997). However, using SDSL, individual sites within a given protein structure can be studied according to denaturant unfolding and information on the stability of both membrane-embedded and solvent-exposed domains can be obtained (Klug et al., 1995; Liu & Zhou, 1995; Gibney et al., 1997).

FepA is an 81 kDa ligand-gated receptor responsible for transporting the ferric enterobactin complex (FeEnt) across the outer membrane of *Escherichlia coli* and other gram-negative bacteria. It is proposed to form a β-barrel structure with a large extracellular surface loop occluding the channel opening and acting as the ligand binding site (Murphy et al., 1990). The β-barrel proposal is

Reprint requests to: Jimmy B. Feix, Biophysics Research Institute, Medical College of Wisconsin, 8701 Watertown Plank Road, Milwaukee, Wisconsin 53226; e-mail: jfeix@mcw.edu.

Abbreviations: ΔG_U, free energy of unfolding; ESR, electron spin resonance; Gdn-HCl, guanidine hydrochloride; MTSL, (1-oxy-2,2,5,5-tetramethylpyrroline-3-yl)methyl methanethiosulfonate spin label; SDSL, site-directed spin labeling.

based on hydrophobicity analysis, which verifies the lack of long hydrophobic stretches indicative of transmembrane α-helices, and comparison to the currently crystallized porins (Cowan et al., 1992; Schirmer et al., 1995). Recently, the β-sheet structural content was confirmed by our group with an entire β-strand studied and mapped according to depth in the bilayer using SDSL (Klug et al., 1997). We have also previously characterized a residue located in the ligand-binding domain according to denaturant unfolding and found the region to cooperatively unfold both in Gdn-HCl and urea (Klug et al., 1995). In this work, we extend the mapping of the confirmed β-strand in FepA to a region spanning from the periplasm up into the ligand-binding domain and investigate the unfolding of these residues.

Results

β-Strand characterization

The region of FepA containing residues Q245 to Y253 was previously characterized using SDSL and determined to be involved in a transmembrane β-strand (Klug et al., 1997). This confirmed the proposal of β-sheet secondary structure in FepA and laid the framework for further analysis of FepA structure and function. More recently, we extended the characterization of this β-strand by four additional residues to extend slightly beyond the rigid β-strand structure.

Results obtained for the β-strand residues in reconstituted liposomes from power saturation experiments are summarized in Table 1. The four newly characterized residues are L244, S254, R255, and Q256. Higher accessibility to O_2, as measured by both $\Delta P_{1/2}$ and the dimensionless accessibility parameter Π, indicates exposure to the hydrophobic region of the bilayer, while increased accessibility to the polar relaxation agent NiEDDA indicates exposure to either the interior of the transmembrane channel or the external aqueous phase. Depth calculations (see Materials and methods) were made for the lipid-exposed residue, R255C, and it was determined to be located in the polar headgroup region of the lipid bilayer at 1.4 Å. This is entirely expected, as residue Y253C was estimated at about 8 Å, and alternate residues in an ideal β-sheet are 6.8 Å apart.

The periodicity in the dimensionless Π parameter with respect to oxygen and NiEDDA (Fig. 1) is markedly out-of-phase between residues Q245C and Y253C, as noted earlier (Klug et al., 1997). However, it is also noteworthy that beyond these residues, the periodicity becomes in-phase, indicating the ends of the strand. Thus, residue L244C appears to reside in a periplasmic β-turn, while S254C, R255C, and Q256C end the strand and become part of the ligand-binding loop region. Thus, an entire region spanning the membrane from the ligand-binding loop domain to the base of the β-barrel is now completely characterized according to depth measurements and ready for further structural analysis.

Table 1. *Accessibility parameters and depth calculations*[a]

Mutant	$\Delta P_{1/2}$ (O_2)[b]	$\Delta P_{1/2}$ (CROX)	$\Delta P_{1/2}$ (NiAA)	$\Delta P_{1/2}$ (NiEDDA)	Φ	Depth (Å)
L244C	2.58	−0.02	1.15	1.08	0.87	—
Q245C[d]	2.46	0.92	1.62	1.61	0.42	5.1
S246C[d]	1.47	3.77	>20[c]	>20[c]	—	—
L247C[d]	2.99	1.31	1.07	0.77	1.36	8.4
E248C[d]	2.22	2.97	3.76	4.05	−0.60	—
L249C[d]	2.61	0.46	0.56	0.10	3.30	15.2
E250C[d]	2.16	−0.05	0.15	0.97	0.80	—
A251C[d]	2.28	0.19	1.10	0.28	2.11	11.1
G252C[d]	1.36	0.31	0.73	0.87	0.62	—
Y253C[d]	2.08	0.53	1.23	0.66	1.15	7.7
S254C	1.32	1.70	1.85	0.45	1.08	—
R255C	1.99	1.39	5.39	3.70	−0.62	1.4
Q256C	1.33	0.55	0.78	0.85	0.45	—

[a]CW power saturation parameters reflecting accessibility to paramagnetic broadening agents and bilayer depth calculations for MTSL-labeled cysteine mutants of FepA in liposomes.

[b]$\Delta P_{1/2}$ values were obtained in the presence of air (20% oxygen), 20 mM CROX, 20 mM NiAA, or 200 mM NiEDDA. Φ values and depth calculations were obtained using the equations described in Materials and methods.

[c]S246C did not saturate in the presence of either of the Ni(II) compounds used.

[d]Data previously published in Klug et al. (1997) shown for completeness.

Guanidine-HCl effects

Seven MTSL-labeled cysteine mutants comprising the aqueous exposed face of the above characterized β-strand in FepA were analyzed according to their unfolding characteristics in Gdn-HCl using SDSL ESR. In addition, a lipid-exposed site was analyzed for comparison between faces of the β-strand. Samples were prepared and run in the presence of detergent, as FepA has been previously shown to retain its native structure and function in Triton X-100 micelles (Hollifield & Neilands, 1978). Samples were incubated at room temperature for 24 h prior to collecting ESR spectra in order to obtain equilibrium denaturation data (Klug et al., 1995).

The spectra for each mutant after 24 h at room temperature in the absence of denaturant are presented in Figure 2. The low-field peak indicates an immobilized environment for the spin label, which is indicative of tightly packed local protein structure. The appearance of the more mobile component, as indicated in Figure 2 by an arrow, indicates freer motion of the spin label, which arises

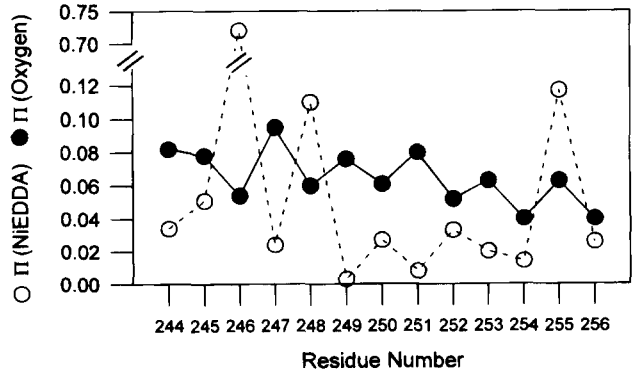

Fig. 1. Variation of the accessibility parameter Π as a function of spin label position in FepA. The biphasic out-of-phase periodicity in Π for oxygen and NiEDDA is indicative of β-sheet secondary structure. The ends of the strand can be recognized by the accessibilities to both oxygen and NiEDDA becoming in-phase.

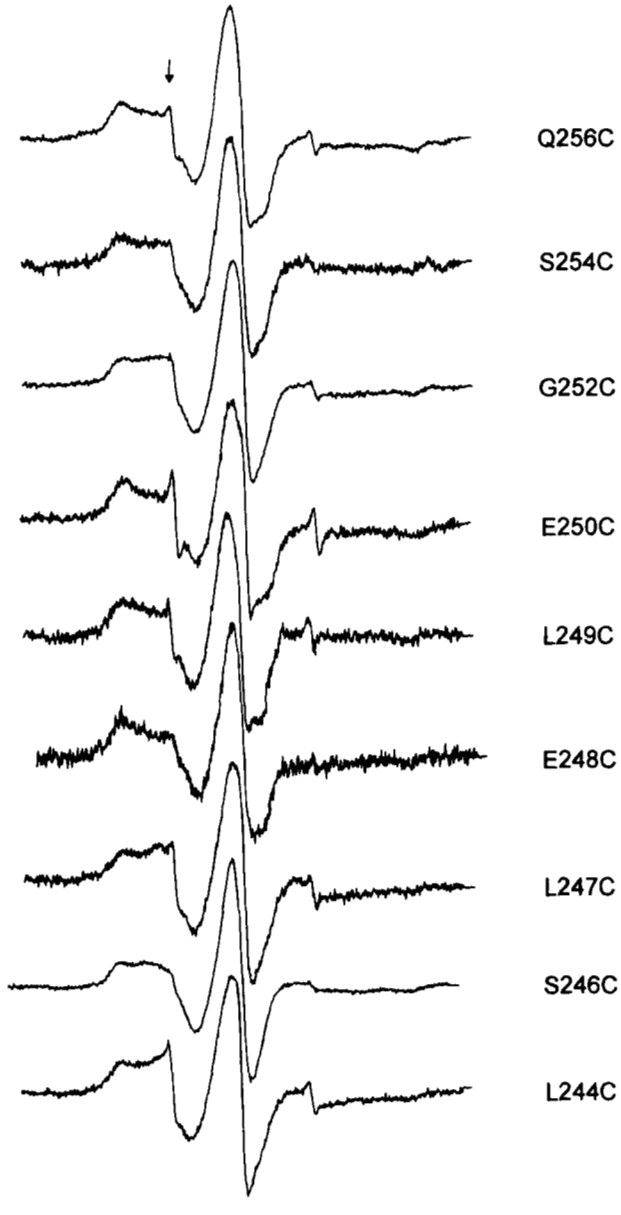

Fig. 2. ESR spectra of control (0.0 M Gdn-HCl) samples run after 24 h at room temperature. The arrow indicates the more mobile component of the spectrum, representing local unfolding.

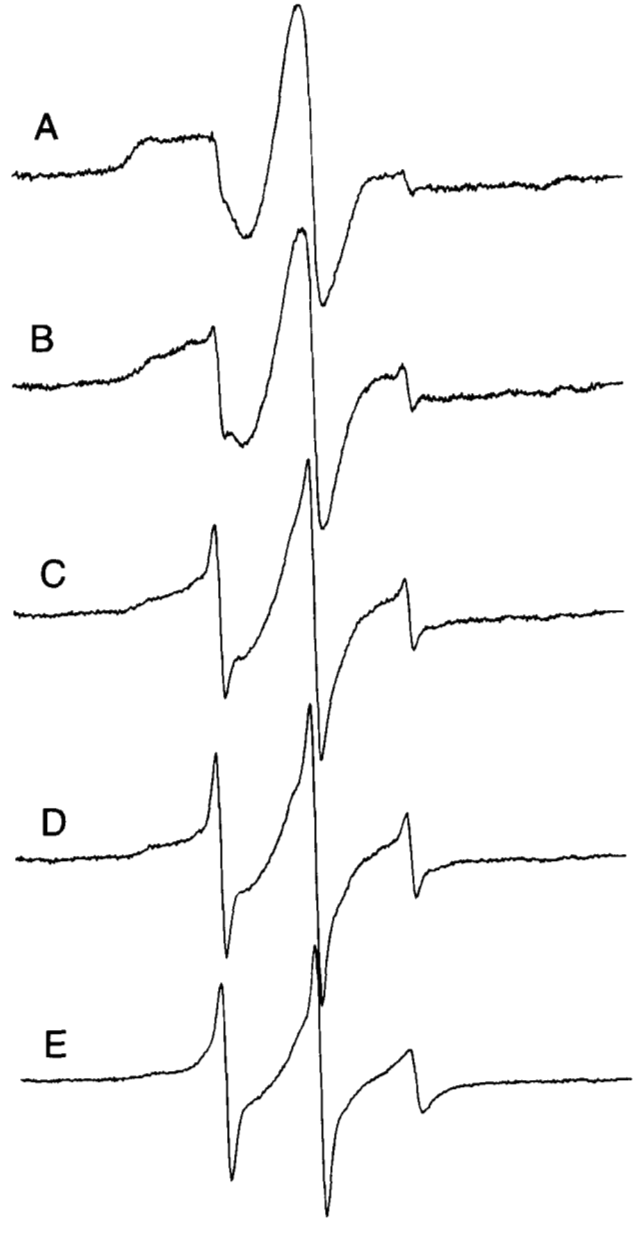

Fig. 3. Example of progressive denaturation as observed by ESR spectra. MTSL-labeled G252C equilibrated at room temperature for 24 h in (**A**) 0.0 M, (**B**) 1.25 M, (**C**) 1.5 M, (**D**) 1.75 M, and (**E**) 4.0 M Gdn-HCl. The freely mobile component, indicating loss of structural constraints at the site of the label, increases with increasing concentration of Gdn-HCl, while the more immobilized component, indicating native structure, decreases.

due to loss of local tertiary structure at the labeled site. Most sites are only slightly denatured at this point in the absence of denaturant; however, S246C appears to be the most stable of the sites studied at room temperature. Upon the addition of increasing amounts of Gdn-HCl, the sharp component in the ESR spectrum increases and the native, broad low-field signal decreases. This is illustrated in Figure 3, with the progression of G252C from a nearly native to fully denatured spectrum as the concentration of denaturant is increased. By 4.0 M Gdn-HCl, the protein is fully denatured (Klug et al., 1995). The spectra for each mutant in the presence of 4.0 M Gdn-HCl after 24 h are shown in Figure 4. It is noteworthy that the channel exposed residues (Fig. 4A) become more freely mobile than the lipid-exposed residues (Fig. 4B) under fully denaturing conditions.

The amount of denatured component in each spectrum can readily be determined using spectral subtraction methods (see Materials and methods). The results of analyzing each mutant according to the percent denatured under varying concentrations of Gdn-HCl are given in Figure 5. All the sites give cooperative unfolding curves with transitions over relatively narrow denaturant concentrations, which is similar to what we previously observed for a residue within the ligand binding domain (Klug et al., 1995). Although the protein is fully denatured by 4.0 M Gdn-HCl, as mentioned above, it can be seen in Figure 4 that not all the sites (especially L249C and L247C) have converted to a completely

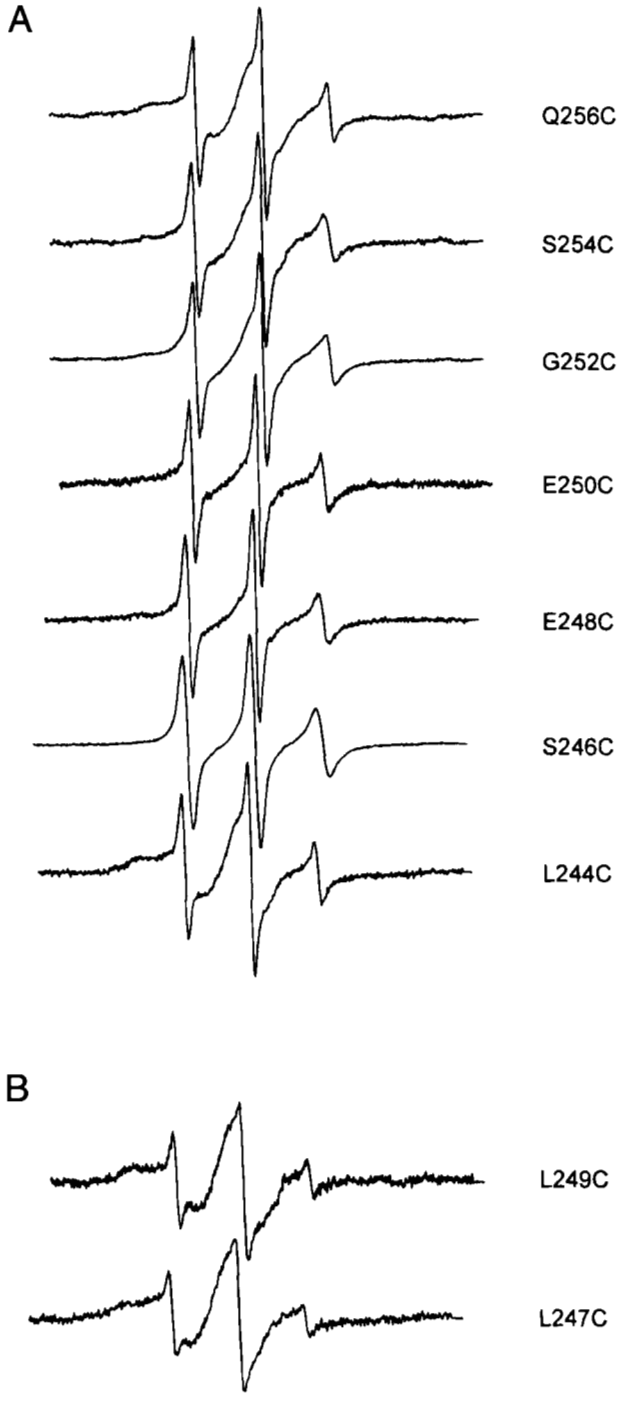

Fig. 4. ESR spectra of (**A**) channel-exposed sites and (**B**) lipid-exposed sites in 4.0 M Gdn-HCl after 24 h.

free environment. The amount of free label was determined by subtracting a freely mobile spectrum from each of the experimental L247C spectra and plotted as open circles in Figure 5. It can be seen that the cooperative unfolding curve shifts to a linear, uncooperative plot. Similar results were seen for L249C, an adjacent lipid-exposed site (data not shown). Yet, when this latter method was employed for the remaining sites, cooperative curves were once again obtained, and when the values were scaled so that the 4.0 M Gdn-HCl percentages matched, the data points overlaid those shown in Figure 5. In addition, CD data also indicate cooperative unfolding (data not shown).

Using a two-state model, the free energy of unfolding (ΔG_U) for each particular site was calculated using two different methods (see Materials and methods for details). The values obtained upon analysis of the curves in Figure 5 are given in Table 2. The first column gives the ΔG_U in the absence of denaturant (ΔG_U°) as calculated by extrapolating to zero denaturant concentration. This method also yields a measure of cooperativity of the unfolding transition, termed m. An alternative, and possibly more reliable, method of calculating ΔG_U° (Kellis et al., 1989) involves calculation of the midpoint of the transition (C_m); these values are also presented in Table 2. We find the two methods agree very well in our studies. Residues S246C–S254C, which are directly involved in the β-strand secondary structure, show a v-shaped relationship in their free energies of unfolding, with the highest energy in the center of the strand at residue E250C. This relation extends into the ligand binding loop region to Q256C, which has the lowest ΔG_U°, while L244C, a periplasmic turn residue, has a higher ΔG_U° than might be expected for an exposed site (see Discussion). Data for L247C show it to have a very low ΔG_U° (~2.00 kcal/mol); although, the fact that this site does not become freely mobile even when the protein is fully denatured may help explain this value and will be discussed below. The cooperativity of the unfolding transition of the central residues, S246C–S254C, is fairly high and peaks at the center with E250C, just as was observed for the free energy of unfolding values. Those positions on the very ends of the strand (L244 and Q256) tend to be less cooperative, with Q256C the least cooperative of the residues studied in this strand. Next, the opposite trend is seen for the transition midpoint values, with L244 and Q256 having higher C_m values than those sites directly involved in the β-strand (Table 2). Thus, sites occupying the center of the aqueous face of the transmembrane strand are more stable and unfold with higher cooperativity than end residues and Q256C in the adjacent surface loop.

Discussion

This study has utilized SDSL to characterize and map additional residues related to a previously characterized β-strand of the ferric enterobactin receptor, FepA (Klug et al., 1997). The high accessibility of L244C to oxygen and low accessibility to the polar reagents indicates that this site is in a restricted, hydrophobic environment. However, the depth of Q245C at about 5 Å into the lipid bilayer indicates that the L244C site is part of the periplasmic turn. Also, as illustrated in Figure 1, the out-of-phase periodicity characteristic of β-sheet secondary structure becomes in-phase at residue L244C, indicating that this site is not a part of the rigid β-strand structure. Further evidence of this site being involved in the turn is the fact that it is directly adjacent to a proline residue. Because proline residues are commonly found in tight β-turns and absent from β-strand secondary structure, we conclude that we have characterized this entire end of the strand into the periplasm. On the extracellular surface, we characterized three additional sites. S254C was expected to be located on the aqueous face of the β-strand and was, therefore, not given a depth estimate, while R255C was estimated at 1.4 Å, which places it in the polar head group region of the bilayer. This is entirely expected as Y253C was calculated to be about 8 Å into the bilayer and alternate residues in an ideal antiparallel β-strand are 6.8 Å apart. Q256C gives lower

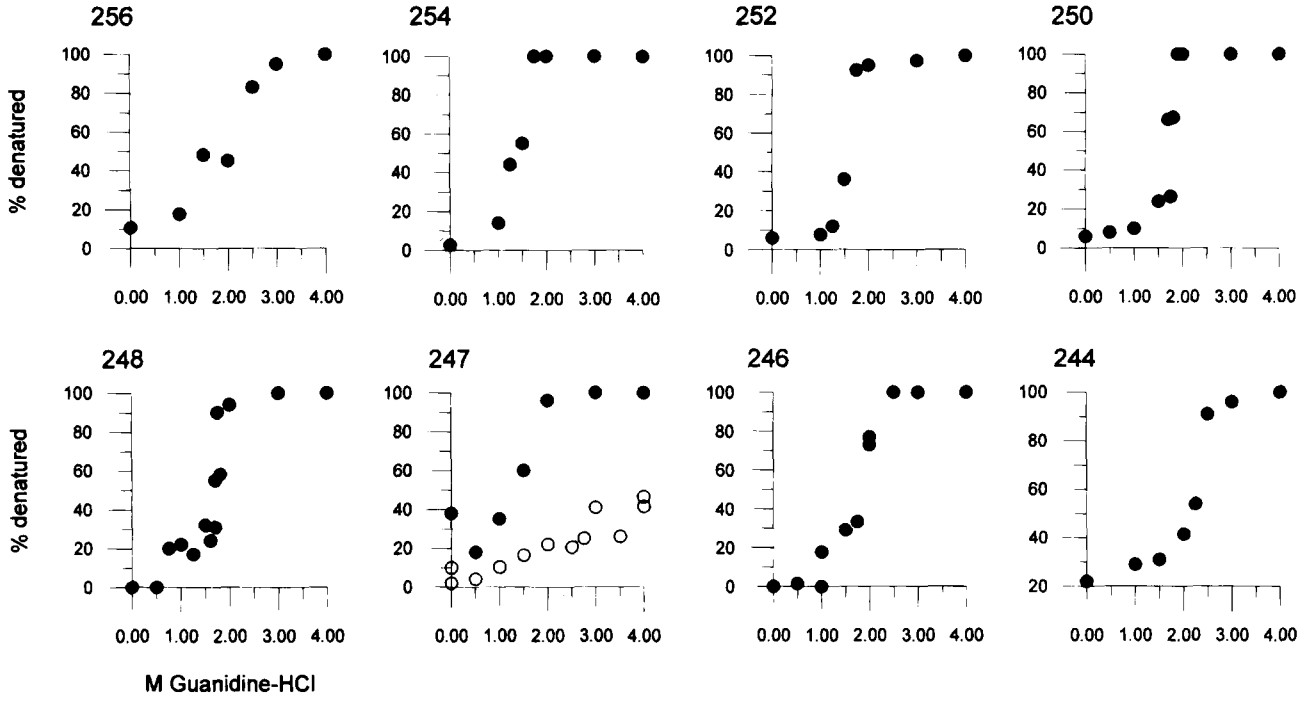

Fig. 5. Gdn-HCl denaturation curves for each mutant as indicated by residue number. The percent of denatured protein was determined as described in Materials and methods using spectra obtained in the presence of 4.0 M Gdn-HCl for spectral subtraction. Open symbols for L247C represent an alternative method of analysis.

exposure to any of the reagents used than expected if it were free of the β-strand structure and involved in the large extracellular loop. However, the ligand-binding loop is so large that significant hydrophobic and tertiary interactions must be occurring to order and structure this loop, so it is not entirely surprising that this site is less accessible than those sites exposed to the aqueous face of the channel along the β-strand. That the alternate periodicity of 2.0 in Figure 1 for the residues up to Y253C falls off and becomes in-phase for S254C, R255C, and Q256C further suggests that these residues mark the end of the strand and begin the extracellular loop domain. Consequently, we now have an entire strand characterized from the periplasm to the extracellular ligand binding domain.

Table 2. *Thermodynamic parameters for the guanidine-HCl unfolding of FepA β-strand mutants*[a]

Mutant	ΔG_U° (kcal/mol)[b]	ΔG_U° (kcal/mol)[c]	m (kcal/mol/M)	C_m (M)
256	2.28	2.50	1.31	1.91
254	5.94	5.95	4.61	1.29
252	7.93	7.92	5.28	1.50
250	9.79	9.04	5.76	1.57
248	6.83	6.73	4.08	1.65
246	7.77	7.45	4.21	1.77
244	6.88	7.41	3.25	2.28

[a] ΔG_U° is the free energy of unfolding in the absence of denaturant calculated using the linear extrapolation method[b] and mC_m[c]. C_m is the midpoint of the equilibrium unfolding transition and m, the slope of the linear extrapolation, is a measure of the cooperativity of the unfolding transition.

We have also utilized SDSL ESR to probe the unfolding of individual sites within the transmembrane β-strand described above. The even-numbered residues in this strand face the inside of the channel and show cooperative equilibrium unfolding curves, with a sharp transition from native to denatured. In contrast, the residue studied that faces the lipid bilayer gives both cooperative and uncooperative unfolding curves, depending on the method utilized for analysis, clearly indicating a different structural environment.

It is necessary to keep in mind that each individual site is being probed as the entire protein unfolds and that local structure is observed. For this reason, the fact that each site studied does not appear to convert from an immobilized environment to a completely free environment upon full denaturation of the protein gives insight into the local structure surrounding the site within the unfolded protein. Specifically, the sites at the ends of the strands, Q256C, S254C, and L244C do not appear to be in a completely free environment when the protein is fully denatured (Fig. 4A). To start, S254C and Q256C have a small amount of immobilized component left in their 4.0 M Gdn-HCl spectra, which may be explained by the fact that they are at the interface between a rigid β-strand structure and a large ligand binding domain containing a significant amount of hydrophobic sites compared to extracellular eukaryotic membrane receptor loops. Such a location is not always freely exposed to the aqueous phase because unfolded states are random orientations of the residues. More prominently, the fully denatured L244C spectrum shows that less than 50% of the spins are in a free environment. This is likely due to its position in both the amino acid sequence and the secondary structure of the protein, as this site appears to be involved in a tight β-turn and neighbors a proline residue. The involvement of this residue in a β-turn may help explain its high C_m, because the β-barrel structure is a very

stable conformation and most likely unfolds at higher denaturant concentrations, and its location adjacent to a rigid proline residue may help explain the number of labels still quite immobilized. To a further extreme, residues L249C and L247C have a very limited number of free labels under 4.0 M Gdn-HCl conditions (Fig. 4B), leaving the majority of the labels attached to these sites very immobilized, as seen for the same spectra in the absence of denaturant. This is most likely explained by the fact that these two residues are located within the rigid β-barrel structure and are exposed to the hydrophobic face of the strand. These sites may tend to remain in a hydrophobic environment due to the nature of the surrounding residues in the β-strand and, therefore, are not exposed to the aqueous phase or to an environment where the spin label can freely rotate, causing their 4.0 M Gdn-HCl spectra to remain relatively unchanged from the control spectra in the absence of Gdn-HCl. Although the entire protein may be globally unfolded, these sites appear to remain in a locally restricted environment.

For those sites that did not convert from an immobilized to a completely free environment, two different methods for analyzing the amount of denatured component are possible. The first involves the assumption that the spectrum recorded after 24 h at room temperature and in the presence of 4.0 M Gdn-HCl (Fig. 4) represents the environment and motion of the site upon full denaturation of the protein. This appears to be a valid assumption based on the data points observed for the curves, where the values approaching 4.0 M Gdn-HCl tend to level off, indicating the 4.0 M Gdn-HCl value to be fully denatured. Furthermore, a previous denaturation study using urea and SDS-PAGE shows the progressive unfolding of FepA, and by 8.0 M urea the protein was fully denatured (Klug et al., 1995). Because Gdn-HCl is approximately twice as strong a denaturant as urea (Pace, 1986), we can safely argue that the whole protein is fully denatured by 4.0 M Gdn-HCl. Thus, based on this technique, using the spectrum for each individual mutant in 4.0 M Gdn-HCl and assuming a two-state model between native and denatured, all of the mutants studied in this strand show cooperative binding curves and produce the free energies of denaturation presented in Table 2. However, for those sites that do not show freely mobile spectra in the presence of 4.0 M Gdn-HCl, an alternative method of analysis is to calculate the amount of free label only. This requires a freely mobile spectrum with similar lineshapes and is not always feasible. Nonetheless, this was possible for most of the sites with the remaining immobilized component under fully denaturing conditions. Using this second method of analysis, S254C, which has very nearly a completely free spectrum, and L244C, with a significant amount of fairly immobilized component remaining at 4.0 M Gdn-HCl, both showed cooperative curves that overlaid those obtained with the first method when scaled to match the final data points. This clearly shows the cooperative unfolding of these sites regardless of the method of analysis. Yet, when only the free label was subtracted out of the denatured L249C spectrum, a linear, uncooperative relationship was obtained (open circles in Fig. 5). It seems reasonable to expect that the two curves would be identical with either method so long as the 4.0 M Gdn-HCl values are scaled, as is the case with the channel-exposed residues, but this does not occur for the lipid-exposed residues. It is interesting that sites adjacent to one another (e.g., E248C and L247C), but on opposite faces of the β-strand, show such dissimilar unfolding characteristics. We conclude that local structure has a strong influence on the unfolding of individual sites.

The possibility of an intermediate state has not been overlooked, although most of the spectra do not show any signs of an additional motional component besides the native and denatured states. Thus, the two-state model appears to be valid for our studies here. If an intermediate were present, our method of detecting the amount denatured gives a pure percentage value for the denatured component and does not depend on the presence of an intermediate. The error in calculation would occur only when assuming that the remaining amount is still native or in the calculation of ΔG°_{U}, which is valid only for two-state systems.

The thermodynamic parameters presented in Table 2 for the alternate residues studied show interesting trends that add insight into the stability of various domains of the FepA structure. The residues comprising the rigid β-strand secondary structure (i.e., S246C–S254C) have fairly similar transition midpoints, with a slight decrease as they approach the ligand binding domain. However, L244C and Q256C, the extreme ends of the strand, both show higher C_m values, indicating greater stability at these sites. The amount of denaturant necessary to unfold roughly half the label attached to each site gives an indication as to the approximate stability of that site in the protein structure. Next, the cooperativity of the unfolding transition, measured by m, tends to be highest near the center of the strand and tapers off toward the ends, forming a bell-shaped relationship between cooperativity and strand location. Q256C is especially uncooperative, as can been seen in Figure 5 even without quantitative analysis (it has an m value significantly lower than the others in this study), and may be due to its position within the protein structure (at the strand/loop interface) as discussed above. Similarly, the free energies of unfolding tend to follow the same trend as the cooperativity values but with a sharper v-shaped relationship, having higher ΔG°_{U}s at the center of the strand and lower ΔG°_{U}s toward the ends. Again, L244C and Q256C are by far the slowest and hardest sites to unfold, with Q256C having the lowest cooperativity and L244C, on the opposite end of the strand, requiring the most denaturant to cause the unfolding transition. This may be explained as above, due to their positions in the secondary and tertiary structure of the protein. Because L244C is positioned adjacent to a proline and appears to be involved in a tight β-turn, it is not surprising that this site is so stable. Also, it is likely that because the β-barrel conformation is very stable, the β-turns would be one of the last sections of the protein to unfold.

In conclusion, the initial work on the complete characterization of a β-strand in FepA not only lays the ground work for further analysis of this strand, which may be involved in some sort of signaling mechanism due to the requirement of inner membrane accessory proteins upon the addition of ligand, but also defines the ends of the strand so that further analysis of an adjacent strand and the ligand-binding domain can be carried out. In addition, we conclude from our Gdn-HCl denaturation studies on the individual residues involved in this β-strand that local environment has a significant impact on loss of structure at each site.

Materials and methods

Site-directed mutagenesis and protein purification

Single cysteine substitutions were created and verified as described previously (Klug et al., 1997). Protein was purified from *E. coli* RWB18-60 harboring a pUC19-based plasmid encoding the

FepA gene as previously published (Neidhardt et al., 1974; Fiss et al., 1982; Klug et al., 1995).

Site-directed spin labeling

The purified protein was specifically labeled at the introduced cysteine residue with the sulfhydryl-specific spin label (1-oxy-2,2,5,5-tetramethylpyrroline-3-yl)methyl methanethiosulfonate (MTSL, Fig. 6, Reanal, Budapest, Hungary) at a twofold to tenfold molar excess overnight at 4 °C. The two native cysteines in FepA have been shown to be involved in a disulfide bond and are not amenable to spin labeling without the addition of a thiol reducing agent (Liu et al., 1994).

Sample preparation

Protein was reconstituted into liposomes containing 5:1 egg L-α-phosphatidylcholine:1-palmitoyl-2-oleoylphosphatidylglycerol with a lipid:protein molar ratio greater than 800:1, as described previously (Klug et al., 1997). NiAA and CROX (potassium tris-(oxalato)chromate], paramagnetic agents used in CW saturation liposome samples, were from Aldrich Chemical Co. (Milwaukee, Wisconsin). NiEDDA was a gift from Dr. C. Altenbach. Samples for unfolding analysis contained spin labeled protein in 20 mM MOPS and 2% Triton X-100, pH 7, diluted with the appropriate amount of 8.0 M Gdn-HCl in 20 mM MOPS/2%Triton to give the desired final concentration of denaturant. Samples were allowed to come to equilibrium at room temperature for 24 h. MOPS, Triton X-100, and Gdn-HCl were from United States Biochemical (Cleveland, Ohio).

Electron spin-resonance spectroscopy

ESR spectroscopy was performed on a Varian E-102 Century series X-band spectrometer (Varian Associates Inc., Palo Alto, California) and data collected using the VIKING software package (National Biomedical ESR Center, Milwaukee, Wisconsin). CW saturation experiments were carried out on liposome samples contained in a gas-permeable TPX capillary (Popp & Hyde, 1981) using a 1.25 G modulation amplitude and varying microwave powers (typically 0.1–36 mW). Denaturation samples were run in a TE102 rectangular cavity using glass capillaries at 10 mW microwave power, 1.0 G modulation amplitude, a 2-min scan time, and a 100 G scan width. Spectra were typically signal averaged 16 times.

CW saturation data analysis

The peak-to-peak intensity (A) of the first derivative center resonance line ($m_I = 0$) was measured and plotted against the square root of the incident microwave power ($P^{1/2}$). The data points on this curve were fit in Microcal Origin (Microcal Software, Inc., Northampton, Massachusetts) to the following equation:

$$A = IP^{1/2}[1 + (2^{1/\epsilon} - 1)P/P_{1/2}]^{-\epsilon} \quad (1)$$

(Altenbach et al., 1994), where I is a scaling factor, ϵ is a homogeneity factor, and $P_{1/2}$, the half-saturation parameter, is the power at which the signal intensity is half that which it would be in the absence of saturation. The change in $P_{1/2}$ in the presence (e.g., O_2, CROX, NiEDDA, or NiAA) and absence (under N_2) of a given relaxation agent, $\Delta P_{1/2}$, is directly proportional to the local concentration of agent at the site of the spin label (Altenbach et al., 1989), therefore presenting a useful parameter for accessibility of each site to various types of reagents. The $\Delta P_{1/2}$ values obtained in the presence of O_2 and NiEDDA can be utilized to calculate depth measurements within the lipid bilayer using the following equation:

$$\Phi = \ln[\Delta P_{1/2}(O_2)/\Delta P_{1/2}(\text{NiEDDA})] \quad (2)$$

also defined by Altenbach et al. (1994) and the calibration equation determined by our lab for the specific liposome system employed in this study:

$$\text{depth (Å)} = 3.56\Phi + 3.62 \quad (3)$$

(Klug et al., 1997). The Π values are dimensionless accessibility parameters, defined by normalizing the $\Delta P_{1/2}$ values to the width of the center line and the $P_{1/2}$ of a DPPH (2,2-diphenyl-1-picrylhydrazyl) standard (Farahbakhsh et al., 1992), that allow $\Delta P_{1/2}$ values obtained to be compared between laboratories. The above information, along with more extensive detail, can be found in Klug et al. (1997).

Denaturation analysis

To obtain percent denatured values from each spectrum, spectral subtraction was used in which the 4.0 M Gdn-HCl spectrum was subtracted from each of the composite spectra using the program Sumspec (National Biomedical ESR Center, Milwaukee, Wisconsin) as previously published (Klug et al., 1995). The Gdn-HCl concentration versus percent denatured was plotted and two methods for determining the free energy of unfolding of the denatured protein were used. The first method involves the linear extrapolation method (reviewed in Pace, 1986) and utilizes the following equations:

$$K_{dn} = f_D/f_N \quad (4)$$

for a two-state equilibrium between native (f_N) and denatured (f_D) protein, and the Gibbs free energy of unfolding is defined as

$$\Delta G_U = -RT \ln K_{dn} \quad (5)$$

where R is the gas constant and T is absolute temperature. ΔG_U varies linearly with denaturant concentration and can be extrapolated to zero denaturant concentration to give

$$\Delta G_U^\circ = \Delta G_U + m[\text{denaturant}] \quad (6)$$

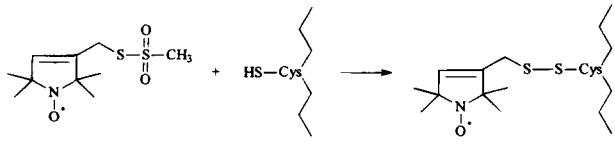

Fig. 6. Sulfhydryl-specific spin labeling with MTSL. The methanethiosulfonate spin label (MTSL) reacts exclusively with the free sulfhydryl group on the substituted cysteine residue.

where m is the slope of the linear extrapolation. Gdn-HCl unfolding curves and linear extrapolations were fit in Microcal Origin (Microcal Software, Inc., Northampton, Massachusetts). The second method involves the midpoint of the transition from native to denatured, C_m, and has been noted that it is possibly a more reliable quantitation (Kellis et al., 1989). The simple relation, $\Delta G^\circ_U = mC_m$, results from the fact that at 50% denaturation, $K_{dn} = 1$. Both methods were utilized in our studies and were found to give values in close agreement.

Acknowledgments

Research in this paper is supported by NIH Grants GM51339, GM22923, and RR011008.

References

Ahmad F, Bigelow CC. 1982. Estimation of the free energy of stabilization of ribonuclease A, lysozyme, α-lactalbumin, and myoglobin. *J Biol Chem 257*:12935–12938.

Altenbach C, Flitsch SL, Khorana HG, Hubbell WL. 1989. Structural studies on transmembrane proteins. 2. Spin labeling of bacteriorhodopsin mutants at unique cysteines. *Biochemistry 28*:7806–7812.

Altenbach C, Greenhalgh DA, Khorana HG, Hubbell WL. 1994. A collision gradient method to determine the immersion depth of nitroxides in lipid bilayers: Application to spin-labeled mutants of bacteriorhodopsin. *Proc Natl Acad Sci USA 91*:1667–1671.

Cowan SW, Schirmer T, Rummel G, Steiert M, Ghosh R, Pauptit RA, Jansonius JN, Rosenbusch JP. 1992. Crystal structures explain functional properties of two *E. coli* porins. *Nature 358*:727–733.

Farahbakhsh ZT, Altenbach C, Hubbell WL. 1992. Spin labeled cysteines as sensors for protein-lipid interaction and conformation in rhodopsin. *Photochem Photobiol 56*:1019–1033.

Feix JB, Klug CS. 1998. Site-directed spin labeling of membrane proteins and peptide-membrane interactions. In: Berliner LJ, ed. *Spin labeling: The next millennium*. New York: Plenum. pp 251–281.

Fiss EH, Stanley-Samuelson P, Neilands JB. 1982. Properties and proteolysis of ferric enterobactin outer membrane receptor in *Escherichia coli* K12. *Biochemistry 21*:4517–4522.

Gibney BR, Johansson JS, Rabanal F, Skalicky JJ, Wand AJ, Dutton PL. 1997. Global topology & stability and local structure & dynamics in a synthetic spin-labeled four-helix bundle protein. *Biochemistry 36*:2798–2806.

Hill B, Cook K, Robinson N. 1988. Subunit dissociation and protein unfolding in the bovine heart cytochrome oxidase complex induced by guanidine hydrochloride. *Biochemistry 27*:4741–4747.

Ho SP, DeGrado WF. 1987. Design of a 4-helix bundle protein: Synthesis of peptides which self-associate into a helical protein. *J Am Chem Soc 109*:6751–6758.

Hollifield WC Jr, Neilands JB. 1978. Ferric enterobactin transport system in *Escherichia coli* K-12. Extraction, assay, and specificity of the outer membrane receptor. *Biochemistry 17*:1922–1928.

Hubbell WL, Altenbach C. 1994. Investigation of structure and dynamics in membrane proteins using site-directed spin labeling. *Curr Opin Struct Biol 4*:566–573.

Kellis JT Jr, Nyberg K, Fersht AR. 1989. Energetics of complementary side-chain packing in a protein hydrophobic core. *Biochemistry 28*:4914–4922.

Klug CS, Su W, Feix JB. 1997. Mapping of the residues involved in a proposed β-strand located in the ferric enterobactin receptor FepA using site-directed spin labeling. *Biochemistry 36*:13027–13033.

Klug CS, Su W, Liu J, Klebba PE, Feix JB. 1995. Denaturant unfolding of the ferric enterobactin receptor and ligand-induced stabilization studied by site-directed spin labeling. *Biochemistry 34*:14230–14236.

Kragelund BB, Robinson CV, Knudsen J, Dobson CM, Poulsen FM. 1995. Folding of a four-helix bundle: Studies of acyl-coenzyme A binding protein. *Biochemistry 34*:7217–7224.

Lau FW, Bowie JU. 1997. A method for assessing the stability of a membrane protein. *Biochemistry 36*:5884–5892.

Liu J, Rutz JM, Klebba PE, Feix JB. 1994. A site-directed spin labeling study of ligand-induced conformational change in the ferric enterobactin receptor, FepA. *Biochemistry 33*:13274–13283.

Liu Z-J, Zhou J-M. 1995. Spin-labeling probe on conformational change at the active sites of creatine kinase during denaturation by guanidine hydrochloride. *Biochim Biophys Acta 1253*:63–68.

Matthews BW. 1995. Studies on protein stability with T4 lysozyme. *Adv Protein Chem 46*:249–278.

Mücke M, Schmid FX. 1994. A kinetic method to evaluate the two-state character of solvent-induced protein denaturation. *Biochemistry 33*:12930–12935.

Murphy CK, Kalve VI, Klebba PE. 1990. Surface topology of the *Escherichia coli* K-12 ferric enterobactin receptor. *J Bacteriol 172*:2736–2746.

Neidhardt FC, Bloch PL, Smith DF. 1974. Culture medium for enterobacteria. *J Bacteriol 119*:736–747.

Oikawa K, Lieberman DM, Reithmeier RA. 1985. Conformation and stability of the anion transport protein of human erythrocyte membranes. *Biochemistry 24*:2843–2848.

Pace CN. 1986. Determination and analysis of urea and guanidine hydrochloride denaturation curves. *Methods Enzymol 131*:266–280.

Pace CN, Vanderburg KE. 1979. Determining globular protein stability: Guanidine hydrochloride denaturation of myoglobin. *Biochemistry 18*:288–292.

Popp CA, Hyde JS. 1981. Effects of oxygen on EPR spectra of nitroxide spin-label probes of model membranes. *J Magn Reson 43*:249–258.

Regan L, DeGrado WF. 1988. Characterization of a helical protein designed from first principles. *Science 241*:976–978.

Schirmer T, Keller TA, Wang Y-F, Rosenbusch JP. 1995. Structural basis for sugar translocation through maltoporin channels at 3.1 Å resolution. *Science 267*:512–514.

Yao M, Bolen DW. 1995. How valid are denaturant-induced unfolding free energy measurements? Level of conformance to common assumptions over an extended range of ribonuclease A stability. *Biochemistry 34*:3771–3781.